Modeling the middle Pliocene climate with a global atmospheric general circulation model

Dabang Jiang and Huijun Wang
Nansen-Zhu International Research Centre, Institute of Atmospheric Physics, Chinese Academy of Sciences, Beijing, China

Zhongli Ding
Institute of Geology and Geophysics, Chinese Academy of Sciences, Beijing, China

Xianmei Lang and Helge Drange[1]
Nansen-Zhu International Research Centre, Institute of Atmospheric Physics, Chinese Academy of Sciences, Beijing, China

Received 29 November 2004; revised 7 March 2005; accepted 8 April 2005; published 27 July 2005.

[1] A new climate simulation for the middle Pliocene (ca. 3 Ma BP) is performed by a global grid-point atmospheric general circulation model developed at the Institute of Atmospheric Physics (IAP AGCM) with boundary conditions provided by the U. S. Geological Survey's Pliocene Research, Interpretations, and Synoptic Mapping (PRISM) group. It follows that warmer and slightly wetter conditions dominated at the middle Pliocene with a globally annual mean surface temperature increase of 2.60°C, and an increase in precipitation of 4.0% relative to today. At the middle Pliocene, globally annual terrestrial warming was 1.86°C, with stronger warming toward high latitudes. Annual precipitation enhanced notably at high latitudes, with the augment reaching 33.5% (32.5%) of the present value at 60–90°N (60–90°S). On the contrary, drier conditions were registered over most parts at 0–30°N, especially in much of East Asia and the northern tropical Pacific. In addition, both boreal summer and winter monsoon significantly decreased in East Asia at the middle Pliocene. It is indicated that the IAP AGCM simulation is generally consistent with the results from other atmospheric models and agrees well with available paleoclimatic reconstructions in East Asia. Additionally, it is further revealed that the PRISM warmer sea surface temperature and reduced sea ice extent are main factors determining the middle Pliocene climate. The simulated climatic responses arising from the PRISM reconstructed vegetation and continental ice sheet cannot be neglected on a regional scale at mid to high latitudes (like over Greenland and the Qinghai-Tibetan Plateau, and around the circum-Antarctic) but have little influence on global climate.

Citation: Jiang, D., H. Wang, Z. Ding, X. Lang, and H. Drange (2005), Modeling the middle Pliocene climate with a global atmospheric general circulation model, *J. Geophys. Res.*, *110*, D14107, doi:10.1029/2004JD005639.

1. Introduction

[2] Paleoclimate model simulations are generally used to test whether complex physically-based climate models can appropriately describe the sensitivity to varying internal and external boundary and forcing conditions. The ability to correctly simulate past climates gives confidence in model-based description of future climate changes [*Kohfeld and Harrison*, 2000]. At the same time, model-model and paleodata-model comparisons will, in general, improve model adequacy and provide interpretation of paleoclimatic states and events, respectively.

[3] A variety of climate states have been present in the Earth's history. With the steady increasing concentrations of atmospheric greenhouse gasses [e.g., *Cubasch et al.*, 2001], it is of particular interest to explore warm past climate scenarios that may have some similarities to the expected near future climate state. The middle Pliocene (ca. 3 Ma BP), the most recent interval of geologic time during which global climate was significantly warmer than at present [e.g., *Crowley*, 1996; *Dowsett et al.*, 1996], may provide a unique climate interval to improve our understanding on the operation of a warmer-than-today climate regime. Reconstruction data from various proxies (e.g., marine microfossils, deep sea records, foraminifers, diatoms, ostracods, fossil pollen, plant macrofossil) indicate that the warm middle Pliocene climate was characterized by increased sea surface temperatures (SST) at middle to high latitudes, reduced extent and thickness of ice sheets and sea ice, a sea level rise of at least 25 m, and the presence of warmth or moisture loving vegetation at middle to high latitudes compared with the present [*Dowsett et al.*, 1999, and references therein].

[1] Also at Nansen Environmental and Remote Sensing Centre, Bergen, Norway.

0148-0227/05/2004JD005639$09.00

[4] Since the release of the first reconstruction data set for the middle Pliocene, compiled by the Pliocene Research, Interpretation, and Synoptic Mapping (hereinafter as PRISM) group under the U. S. Geological Survey [*Dowsett et al.*, 1994], five atmospheric general circulation model (AGCM) simulations with prescribed SST have, to the best of our knowledge, been reported: *Chandler et al.* [1994] used the GISS AGCM (8° × 10° horizontal resolution) to reconstruct the Northern Hemisphere middle Pliocene climate with the PRISM 8° × 10° data set [*Dowsett et al.*, 1994]. *Sloan et al.* [1996] utilized the NCAR GENESIS AGCM (about 4.5° × 7.5° resolution) to perform another simulation with the PRISM1 2° × 2° data set [*Dowsett et al.*, 1996; *Thompson and Fleming*, 1996], and to investigate global-scale climate changes at the middle Pliocene. *Haywood et al.* [2000a] used the new PRISM2 2° × 2° data set [*Dowsett et al.*, 1999] and the HadAM3 version of the U. K. Meteorological Office's Unified Model, with the analysis focusing on the regional warming over Europe and Mediterranean. Finally, *Haywood et al.* [2000b] used the PRISM2 2° × 2° data set and examined the global-scale paleoclimate reconstruction of the middle Pliocene climate with the version 3.0 of the UKMO AGCM (2.5° × 3.75°). In addition, *Haywood et al.* [2002b] conducted three sensitivity experiments addressing the East Antarctic ice sheet configuration at the period. At present, there is no definitive evidence for the reasons responsible for the warm Pliocene climate even if increased poleward ocean heat transports may have played an important role in maintaining the climate at the middle Pliocene [e.g., *Cronin*, 1991; *Rind and Chandler*, 1991; *Crowley*, 1996; *Dowsett et al.*, 1996; *Raymo et al.*, 1996; *Billups et al.*, 1998; *Kim and Crowley*, 2000; *Bennike et al.*, 2002].

[5] A central theme in paleoclimate modeling is to let different climate models simulate the same past climate interval to investigate common and different responses to the imposed paleoclimate boundary and forcing conditions [*Joussaume and Taylor*, 2000]. In an attempt to explore the middle Pliocene warm period, the IAP AGCM is used to examine climate response to the latest version of the PRISM2 data set [*Dowsett et al.*, 1999, and personal communication, 2004]. Such an exercise is particularly helpful to address East Asian middle Pliocene climate since the model's present climate is quite representative in this region [e.g., *Bi*, 1993]. The presented model results are then compared with other model products both on a global scale and with paleoclimatic reconstructions in East Asia. At the same time, the isolated influences derived from the PRISM2 compiled SST and sea ice extent, terrestrial vegetation, and continental ice sheet fields are respectively evaluated for the first time. As indicated, East Asian climate are emphasized in this study because East Asian climate changes and paleoenvironmental states during different historical periods, particularly earlier than the Pleistocene, are poorly known [e.g., *An et al.*, 2001; *Ding et al.*, 2000, 2001; *Guo et al.*, 2004].

2. Model, Boundary Conditions, and Experimental Design

2.1. IAP Atmospheric General Circulation Model

[6] The IAP global grid-point atmospheric general circulation model used in this study was developed at the Institute of Atmospheric Physics under the Chinese Academy of Sciences. It has a horizontal grid resolution of 4° in latitude by 5° in longitude and nine levels unevenly spaced in the vertical with the top at 10 hPa. A brief description on the IAP AGCM dynamical framework, physical processes, land surface process schemes was presented by *Jiang et al.* [2003], and more details are given by *Zeng et al.* [1987], *Zhang* [1990], and *Liang* [1996], respectively.

[7] To date, a series of climatic studies have been carried out with the IAP AGCM for over a decade, and the realistic representations of the present day climate state are obtained, especially in East Asia. As an example, Figure 1 shows that observational annual surface temperature distributes band shape along with latitudes and gradually drops northward, at the same time with a large extent of cooling being present over the Qinghai-Tibetan Plateau. In general, the IAP AGCM reproduces the above spatial distribution pattern quite well, although simulated contours are relatively smoother and consequently fails to capture small-scale signals. Quantitative investigation confirms the above because the spatial correlation coefficient (SCC) is high up to 0.98, and root mean square error (RMSE), including partial contribution of lower atmospheric CO_2 concentration (315 ppmv in the control run, ca. 1958), is 2.81°C between simulation and observation in the domain of 70–140°E and 15–60°N. Similarly, the simulated geographical distribution pattern of East Asian annual precipitation, most difficult climatic element to be accurately reappeared in East Asian monsoon region by current models, compares favorably to observation, with the SCC being 0.80. It is also found RMSE reaches 1.18 mm/day, which is due partly to the discrepancies (1–2 mm/day) presented over the Qinghai-Tibetan Plateau. For the IAP AGCM reproducibility to simulate present climatology and climatic variability in more details, go to *Bi* [1993] for an overview. Concerned past climate changes, *Jiang et al.* [2003] recently used the model to examine global climate at the Last Glacial Maximum and indicated that the IAP AGCM integration coincided well with the PMIP [*Joussaume and Taylor*, 1995] models. In addition, the AGCM has been used to explore the mid-Holocene climate in East Asia [e.g., *Wang*, 2002; *Wei and Wang*, 2004].

2.2. Middle Pliocene Boundary Conditions and Experiment Design

[8] The middle Pliocene surface conditions used in this work are the latest version of the PRISM2 2° × 2° digital data set, including monthly SST and sea ice extent, coastline, continental topography, surface vegetation, and continental ice sheet. The data set represents the most complete and detailed global reconstruction of climate and environmental conditions older than the last glacial. As in the work by *Dowsett et al.* [1999], the important features of the PRISM2 data set compared with the present climate are (1) greatly reduced continental ice volume with a small Greenland ice cap being the only continental ice in the Northern Hemisphere, (2) greatly reduced sea ice with the Arctic being seasonally ice free, (3) a positive sea level anomaly of 25 m, (4) increased SST at high latitudes, and (5) expansion of evergreen forests to the margins of the

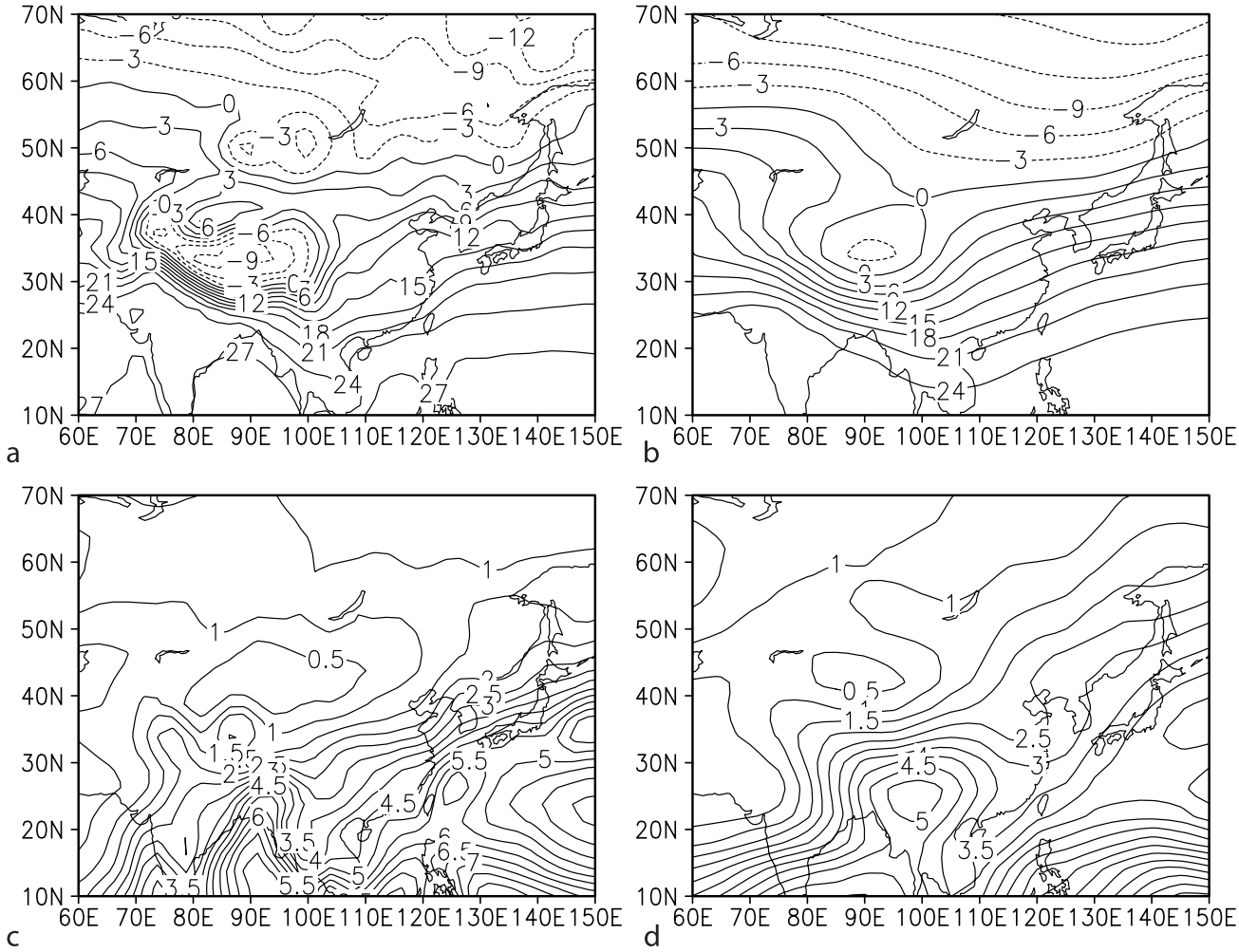

Figure 1. Annual mean surface temperature (°C) derived from the NCEP/NCAR reanalysis data [*Kalnay et al.*, 1996] throughout 1981–1990 (a) against the IAP AGCM ten-year control integration in this study (b), and annual mean precipitation (mm/day) derived from observation [*Xie and Arkin*, 1997] throughout 1981–1990 (c) against the simulation (d).

Arctic Ocean, a reduction of desert area in equatorial Africa and essential elimination of polar desert and tundra regions in the Northern Hemisphere. A small amount of deciduous vegetation occurred at the edge of the Antarctic continent.

[9] Since the atmospheric CO_2 concentration was not too far from 315 ppmv (similar to observation in 1958) at the middle Pliocene [*Rind and Chandler*, 1991], this value was taken for all numerical simulations presented here. Therefore the influences arising from the changes in atmospheric CO_2 level have been excluded, consistent with the studies of *Chandler et al.* [1994] and *Haywood et al.* [2002a]. Except for the above changes, other boundary conditions (e.g., the Earth orbital parameters) in the IAP AGCM were kept at the present configuration.

[10] Five numerical experiments have been carried out, hereafter Exp1 to Exp5, as summarized in Table 1. Exp1 can be regarded as the control run for the present climate and Exp2 as the middle Pliocene climate simulation since all surface boundary conditions are adjusted according to the PRISM2 data set. Furthermore, Exp3–Exp5 have been designed to investigate the isolated contribution of vegetation, continental ice sheet, and SST and sea ice extent to the middle Pliocene climate, respectively.

[11] All simulations were run for 12 years starting from the same initial atmospheric conditions, and the results reported below are ensemble averages for the last 10 years. Statistical significance was assessed by use of a student *t*-test (99% level) applied to differences between every two experiments where the standard deviation and degrees of freedom were based on the averages of the 10 individual

Table 1. Surface Boundary Conditions for the Experiments

Experiment	Monthly SST and Sea Ice Extent, Coastline, Continental Topography, Vegetation, Continental Ice Sheet
Exp1	Modern configuration
Exp2	PRISM2 dataset from U. S. Geological Survey [*Dowsett et al.*, 1999]
Exp3	Same as Exp2, but taking the present day vegetation
Exp4	Same as Exp2, but taking the present day continental ice sheet
Exp5	Same as Exp2, but taking the present day monthly SST and sea ice extent

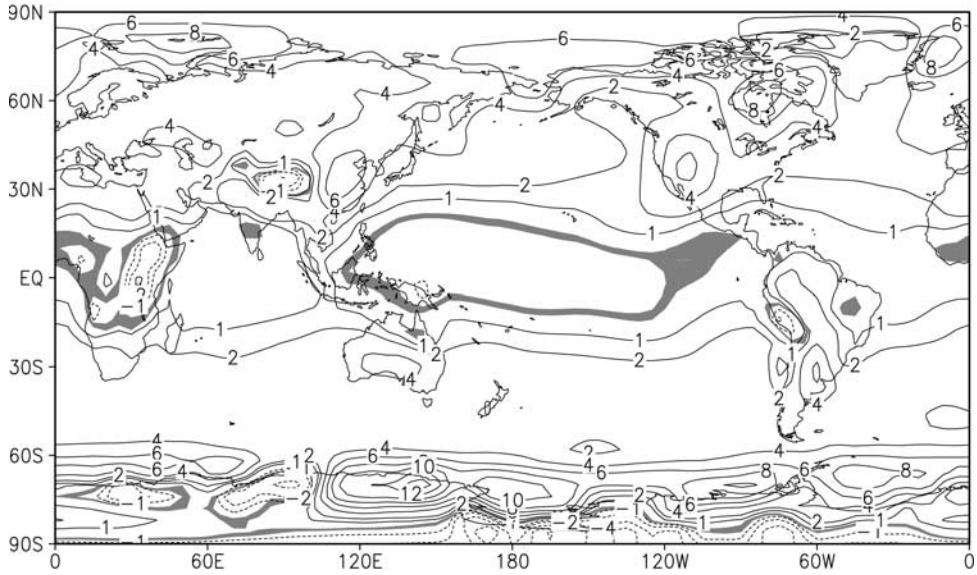

Figure 2. The simulated differences of annual mean surface temperature between the middle Pliocene and the present (Exp2 minus Exp1, unit: °C). Areas with confidence level smaller than 99% are shaded.

years. Additionally, winter denotes December, January, and February, and summer corresponds to June, July, and August throughout this study.

3. Model Results

3.1. Surface Air Temperature

[12] As shown in Figure 2 and Table 2, the middle Pliocene climate differs greatly from the present. A globally annual average surface temperature increase of 2.60°C is obtained, and terrestrial surface temperature rises on average by 1.86°C at the middle Pliocene. However, the obtained warming is not spatially uniform. The warming is strong at 60–90°N, with an annual surface temperature of 4.79°C above the present. The warming maximum is located in the Nordic Seas and the Barents Sea where temperature is 6–10°C higher than at present. The secondary warming maximum (exceeding 6°C) appears around the Baffin Island. At 30–60°N, globally annual mean surface temperature is 3.42°C higher than at present, with terrestrial warming being comparable to oceanic warming. Inversely, cooling is present over parts of the Qinghai-Tibetan Plateau, which can be attributed to higher topography at the middle Pliocene than the present. For instance, the mean topography difference reaches 791 m in the region within 30–34°N and 80–100°E, leading to a cooling of 4.7°C or so if one assumes an atmospheric temperature lapse rate of 0.6°C per 100 m. The obtained warming is smaller at 0–30°N (0.90°C) than that at northern high latitudes. This is mainly caused by the cooling over most parts of northern tropical Pacific with monthly SST values −1.2–0°C below the present values, and by the cooling over the East African rift zone where topography is found to be 500 m higher than today, corresponding to a cooling of about 3°C. Globally annual surface temperature rises on average by 1.22°C, 2.81°C, and 2.59°C at 0–30°S, 30–60°S, and 60–90°S, respectively. On the contrary, the terrestrial surface temperature, as a whole, remains unchanged (−0.005°C in Table 2) at 60–90°S, which can be ascribed to that the strong terrestrial warming at 60–80°S is counteracted by the significant terrestrial cooling, closely associated with the higher topographical height at the middle Pliocene against today (not shown), at 80–90°S.

[13] During winter, globally averaged surface temperature rises on average by 2.45°C, and the warming is generally larger towards the poles (Figure 3). At this time of the year, global terrestrial surface temperature enhances by an average of 2.46°C, with a warming of 2.03°C (3.01°C) in the Northern (Southern) Hemisphere. It is found that except for strong warming over the Nordic and Barents Seas and around the Baffin Island, and an obvious cooling over western parts of Greenland and western North America, the spatial distribution pattern of winter surface temperature difference between the middle Pliocene and the present is generally similar to Figure 2 (not shown).

[14] During summer, globally averaged surface temperature rises by an average of 2.43°C (Figure 3), and the terrestrial warming is 1.43°C. Except for Greenland (6–12°C), summer warming is weaker at northern high latitudes than the average throughout the year (not shown). In addition, a cooling of −1°C to −6°C is found at 80–90°S. As seen in Figure 3, zonally annual, winter and summer

Table 2. Annual Mean Surface Temperature Differences Between the Middle Pliocene and Today (Unit: °C)

	90–60°N	60–30°N	30–0°N	0–30°S	30–60°S	60–90°S	90°N–90°S
Temperature	4.79	3.42	0.90	1.22	2.81	2.59	2.60
Terrestrial temperature	3.35	3.45	1.60	1.31	3.77	−0.005	1.86

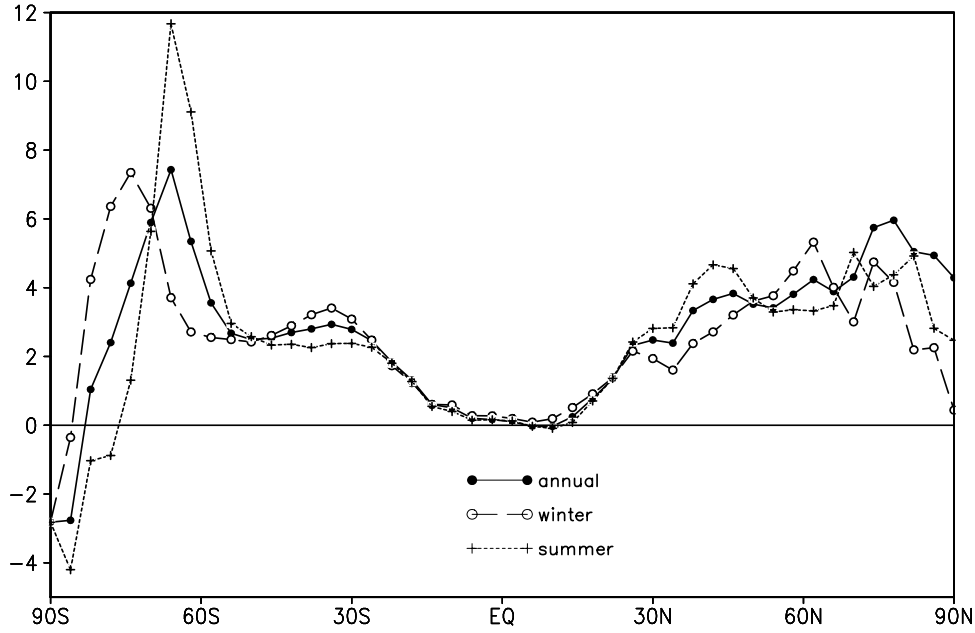

Figure 3. The simulated zonally averaged, annual mean, winter and summer surface temperature differences between the middle Pliocene and the present (Exp2 minus Exp1, unit: °C).

mean surface warming is generally consistent at 50°S–90°N, and disagreement is mainly found at 50–90°S.

[15] It has been amply documented that SST [e.g., *Toracinta et al.*, 2004; *Zhao et al.*, 2004], continental ice sheet [e.g., *Felzer et al.*, 1998; *Clark et al.*, 1999], and vegetation [e.g., *Crowley and Baum*, 1997; *Wang*, 1999] play an important role in the past climate changes. In Exp2, the PRISM2 monthly SST and sea ice extent, continental ice sheet, and vegetation fields have been introduced into the IAP AGCM boundary conditions. To which extent do the above every factor contributes to the middle Pliocene warming? Exp3, Exp4, and Exp5 are used to address this question. It is found that the globally annual mean surface temperature difference between Exp2 and Exp3 is only 0.08°C, with the maximum average difference of 0.23°C at 60–90°N, strongly indicating that the effects of the PRISM2 reconstructed vegetation on the middle Pliocene climate are quite limited. However, it follows from Figure 4 that the vegetation-induced annual warming reaches 0.5–3°C over the Greenland region, 0.5–1°C in the domain bounded by 20°W–60°E and 28–35°N, 0.5–2°C over the Qinghai-Tibetan Plateau, and 0.5–3°C in the region 140–180°E and 70–90°S. These findings imply that the influences of vegetation changes on the middle Pliocene climate

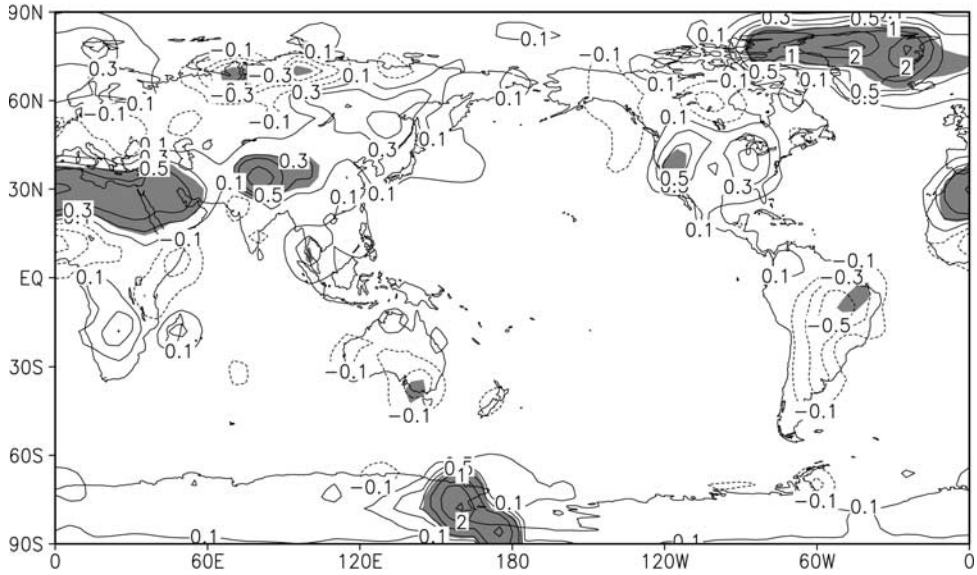

Figure 4. The simulated differences of annual mean surface temperature induced by the reconstructed vegetation (Exp2 minus Exp3, unit: °C). Areas with confidence level exceeding 99% are shaded.

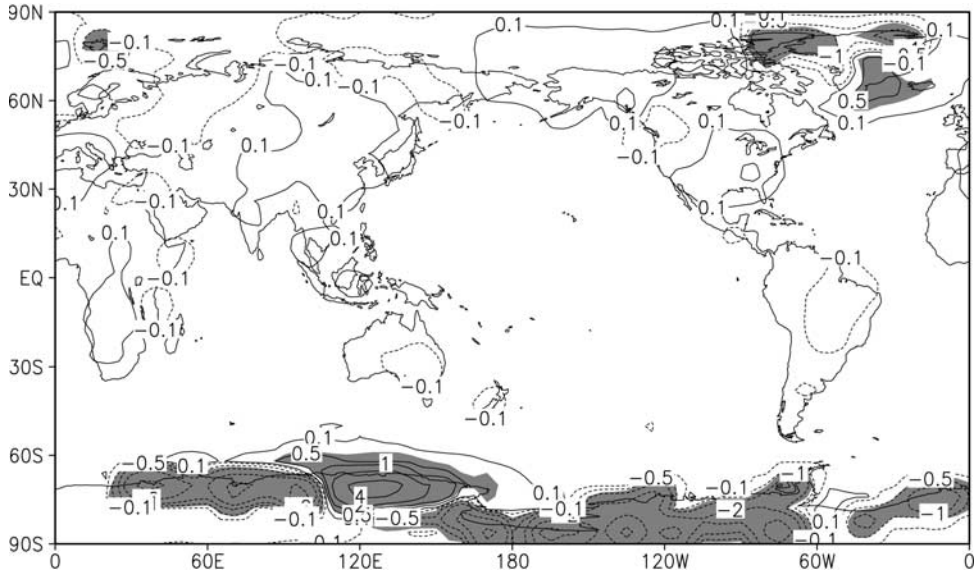

Figure 5. The simulated differences of annual mean surface temperature induced by the reconstructed continental ice sheet (Exp2 minus Exp4, unit: °C). Areas with confidence level exceeding 99% are shaded.

cannot be neglected on a regional scale. As in the work by *Wyputta and McAvaney* [2001], vegetation complicatedly influences climate, primarily through its effect on albedo, evaporation, transpiration, and roughness length, and the resultant changes modify both the heat exchange and water vapor content of the atmosphere. Further investigation reveals that the annual mean albedo as reproduced by the IAP AGCM is reduced over the above four warming regions in Exp2 relative to Exp3, with anomalies ranging from −0.01 to −0.40 (not shown). The maximum albedo decrease is found over Greenland, which is a result of the strongly reduced Greenland ice sheet at the middle Pliocene. In general, a decrease of albedo generally results in increased surface temperature because less solar radiation is reflected back into sky. Additionally, it is noted that the vegetation impact on summer surface temperature is relatively greater than winter in the Northern Hemisphere.

[16] Figure 5 displays that the influences of the PRISM2 continental ice sheet distribution are confined to high latitudes. Globally annual surface temperature increases by 0.5–1°C over southern Greenland and Iceland, and by 0.5–4°C in the domain between 110–170°E and 60–80°S. On the contrary, surface temperature drops by 0.5°C or so over mid to northern Greenland and by about 0.5–2°C over most parts of the circum-Antarctic. Additionally, it is indicated that the reconstructed continental ice sheet leads to temper-

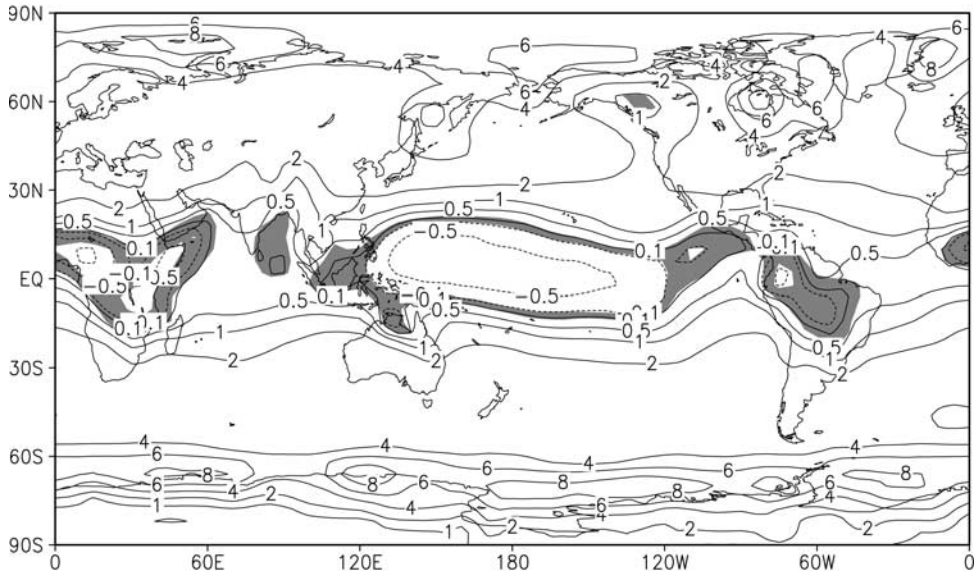

Figure 6. The simulated differences of annual mean surface temperature induced by the reconstructed SST and sea ice extent (Exp2 minus Exp5, unit: °C). Areas with confidence level smaller than 99% are shaded.

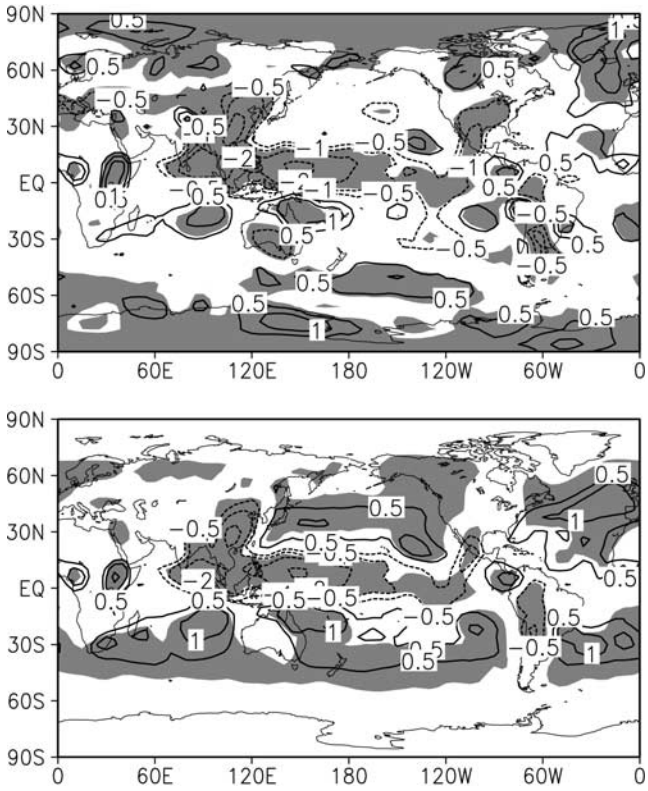

Figure 7. The simulated differences of annual mean precipitation (top) and convective precipitation (bottom) between the middle Pliocene and the present (Exp2 minus Exp1, unit: mm/day). Areas with confidence level exceeding 99% are shaded. See color version of this figure in the HTML.

ature decrease (increase) over and around Greenland in winter (summer) and temperature increase (decrease) over most parts of circum-Antarctic in austral summer (winter) relative to the control integration (not shown).

[17] The impact of the PRISM2 reconstructed SST and sea ice extent on the middle Pliocene climate is pronounced. Globally annual surface temperature difference between Exp2 and Exp5 is 2.73°C, which even exceeds the difference of 2.60°C between Exp1 and Exp2. This finding strongly indicates that the reconstructed monthly SST and sea ice extent are key factors for the middle Pliocene climate simulation in the IAP AGCM. As further seen in Figure 6, globally annual surface temperature is notably higher in Exp2 than in Exp5. The geographical distribution pattern of the temperature difference is, in general, similar to Figure 2. Therefore it can be concluded here that the PRISM2 monthly SST and sea ice extent and associated feedback mechanisms, such as generally warmer SST and reduced sea ice extent corresponding to much more heat transfer into atmosphere, are decisive forcings for the middle Pliocene warmth in the IAP AGCM. If this result can be confirmed by other atmospheric models with similar experiments, paleoclimatologist should pay particular attention on global ocean behaviors at the middle Pliocene.

3.2. Precipitation

[18] At the middle Pliocene, globally annual precipitation is simulated to rise on average by 4.0%, and terrestrial precipitation reaches 112.5%, of the present value. Figure 7 (top) and Table 3 indicate that the geographical distribution of annual precipitation at the middle Pliocene is quite different from that at present. Annual precipitation drops by an average of 0.9% in the Northern Hemisphere and rises by 9.4% in the Southern Hemisphere. The precipitation enhances notably at high latitudes, with the augment reaching 33.5% (32.5%) relative to the control run at 60–90°N (60–90°S). In contrast, drier conditions are registered over most parts at 0–30°N where annual precipitation only accounts for 87.4% of the present. In particular, annual precipitation declines significantly by 0.5–3 mm/day in much of northern tropical Pacific and East Asia. A further examination reveals that the former is mainly derived from notably decreased convective precipitation (Figure 7, bottom). Moreover, decreased convective activity is confirmed in the filed of the outgoing longwave radiation (OLR) at the top of the atmosphere (not shown). It is indicated that OLR enhances significantly by 5–15 W/m^2 in the northern tropical Pacific, especially northwestern tropical pacific, at the middle Pliocene relative to the present, corresponding to a decreased convective activity there. Additionally, East Asian precipitation decrease is found to involve the contribution of both convective and large-scale precipitation.

[19] Investigation of Exp3, Exp4, and Exp5 reveals that the influences of the PRISM2 vegetation and continental ice sheet on annual and seasonal precipitation at the middle Pliocene as simulated in Exp2 is quite limited on a global scale (even on a regional scale), and the precipitation changes displayed in Figure 7 can be attributed to the PRISM2 monthly SST and sea ice extent (Figure 8). The generally lower SST in the PRISM2 data [*Dowsett et al.*, 1999] is generally responsible the increased OLR and reduced convective precipitation in the northern tropical Pacific because lower SST there generally corresponds to an in site weak convective activity and hence to decreased precipitation.

[20] During summer, global precipitation increases by an average of 2.5% at the middle Pliocene relative to today, which is a weaker response than the increase of 5.3% in winter. It is found that summer precipitation drops by about 1–4 mm/day in East Asia, which can be attributed to the significantly decreased East Asian summer monsoon at the middle Pliocene (see the following section). Furthermore, since 40–60 percent of annual precipitation is generally derived from summer over most parts of China at present [*Fu et al.*, 1992], the decrease in summer precipitation

Table 3. Ratio of Annual Mean Precipitation at the Middle Pliocene to the Present

	90–60°N	60–30°N	30–0°N	0–30°S	30–60°S	60–90°S	90°N–90°S
Precipitation	133.5%	100.9%	87.4%	105.9%	104.8%	132.5%	104.0%
Terrestrial precipitation	128.0%	96.0%	96.5%	110.9%	102.8%	190.8%	112.5%

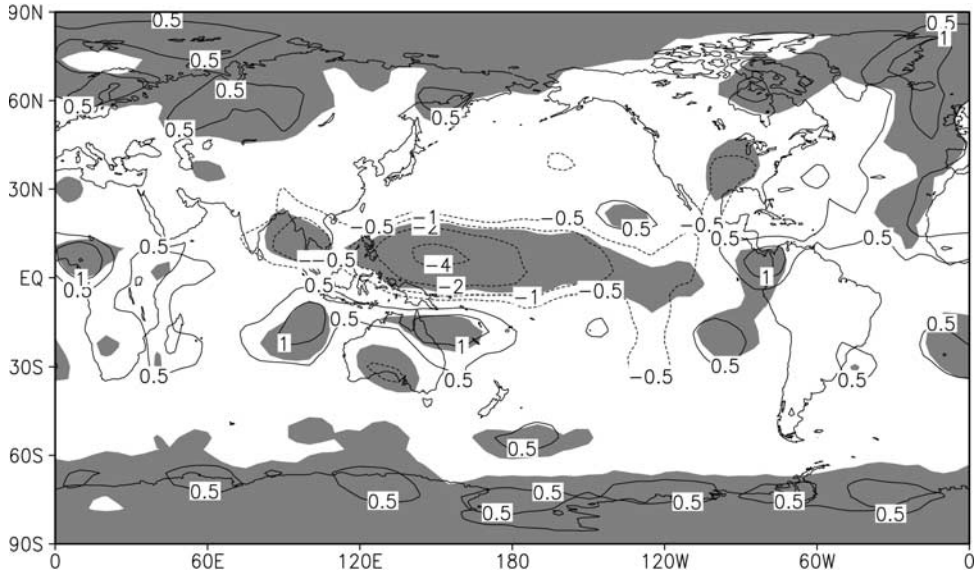

Figure 8. The simulated differences of annual precipitation induced by the reconstructed SST and sea ice extent (Exp2 minus Exp5, unit: mm/day). Areas with confidence level exceeding 99% are shaded.

tends, in general, to annual dryness over mid to eastern China at the middle Pliocene.

3.3. Sea Level Pressure and Atmospheric General Circulation

[21] It is well known that East Asian region is characterized by monsoon climate. During winter, cold high-pressure system generally develop over East Asian continent, and warm low-pressure system are present over the Pacific as a consequence of the difference in the thermal capacity of continent and ocean. The opposite situation is characteristic during summer. The above sea level pressure pattern leads to prevailing northerly (southerly) wind in the low troposphere in winter (summer). During winter at the middle Pliocene, negative sea level pressure anomalies are, in general, present from 120°E westward to 90°W, whereas positive sea level pressure anomalies occur north of 30°S in the region 120°E eastward to 90°W (Figure 9, top), which accords well with the northern hemispheric pattern of *Chandler et al.* [1994]. This implies a weakening of both the cold high-pressure system over East Asian continent and the warm low-pressure system over Pacific Ocean in winter. The latitudinal contrast of sea level pressure between 110°E and 160°E is consequently reduced, resulting in a decreased East Asian winter monsoon at the middle Pliocene compared with the present [*Guo*, 1994].

[22] During summer, positive sea level pressure anomalies extend in much of East Asian continent and the tropical Pacific (Figure 9, bottom). The latitudinal contrast of sea level pressure over East Asia declines to some extent as a result of the larger decrease in magnitude of the warm low-pressure system over East Asian continent compared with the augment of the cold high-pressure system over Pacific. At the same time, the middle Pliocene longitudinal temperature gradient over East Asian continent is reduced because of much stronger warming at high latitudes in summer. Therefore East Asian summer monsoon is weakened at the middle Pliocene.

[23] The differences of the wind field at 850-hPa between the middle Pliocene and present day agree well with the above sea level pressure conception (Figure 10). During winter, southerly wind anomalies are generally present over

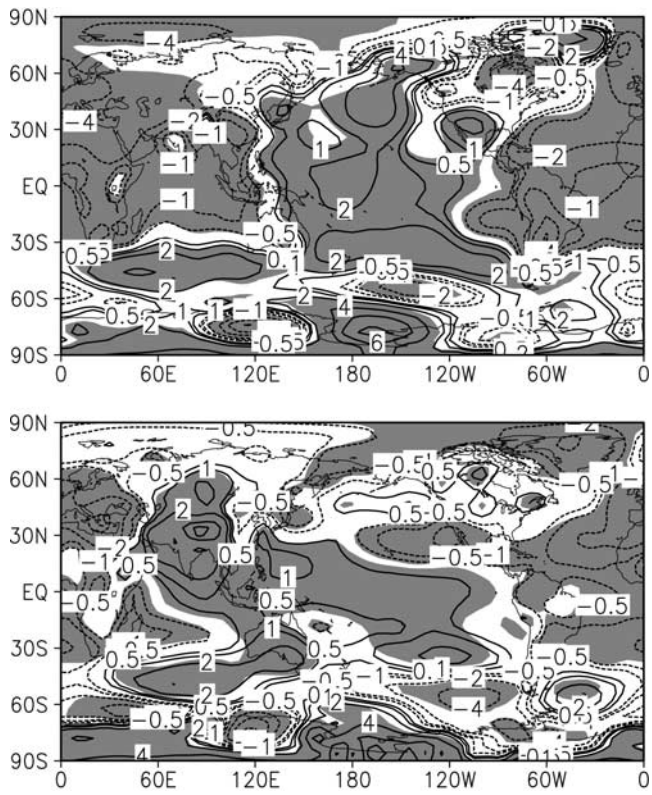

Figure 9. The simulated differences of sea level pressure in winter (top) and summer (bottom) between the middle Pliocene and the present (Exp2 minus Exp1, unit: hPa). Areas with confidence level exceeding 99% are shaded. See color version of this figure in the HTML.

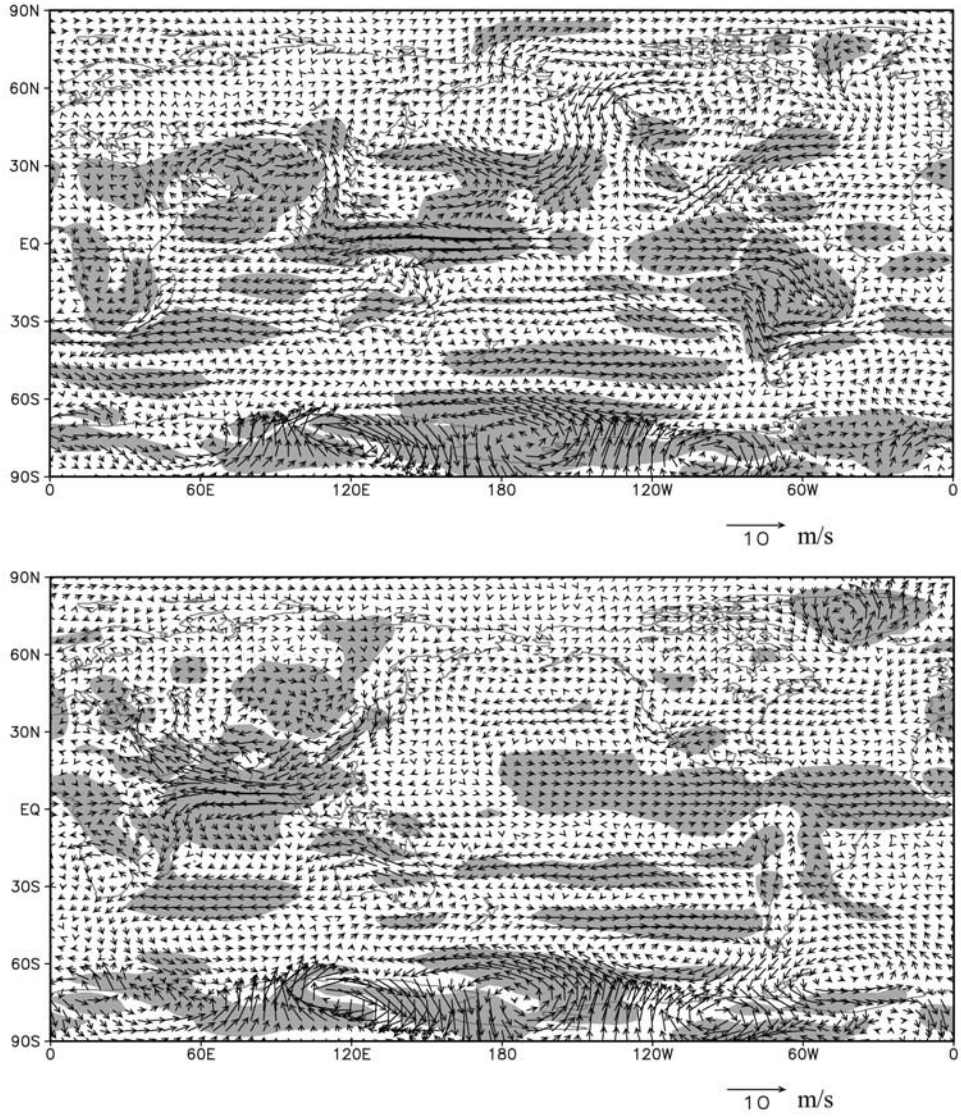

Figure 10. The simulated differences of 850-hPa wind field in winter (top) and summer (bottom) between the middle Pliocene and the present (Exp2 minus Exp1). Areas with confidence level exceeding 99% are shaded. See color version of this figure in the HTML.

East Asia at the middle Pliocene, implying a weak winter monsoon. In the meantime, the anomalous anticyclone over north Pacific is unfavorable for the strength of East Asian winter trough, and the anomalous easterly wind over mid to west tropical Pacific is disadvantageous for northerly wind anomalies over East Asia in winter. During summer, northeasterly wind anomalies are generally present over East Asia, consistent with a weak summer monsoon there. As described by *Tao and Chen* [1987], East Asian summer monsoon is, to lowest order, composed of the subtropical high over western Pacific, the low tropospheric cross-equatorial flow over South China Sea, and the southwest monsoon associated with African monsoon. It can be seen from Figure 10 that decreased East Asian summer monsoon at the middle Pliocene is closely related to the latter. Additionally, it is noted that the differences of surface mean wind as simulated by the UKMO AGCM [*Haywood et al.*, 2000b] are significantly northeasterly in summer and almost remains unchanged in winter over most parts of East Asia, which consequently indicates a weak East Asian summer monsoon at the middle Pliocene. The GISS AGCM produced a slightly intensified summer monsoon and, on the contrary, a clearly weakened winter monsoon in East Asia at the middle Pliocene [*Chandler et al.*, 1994].

[24] The spatial distribution pattern of wind field at 200-hPa at the middle Pliocene is quite similar to the present (not shown). However, Figure 11 exhibits that atmospheric general circulation intensity alters notably in the upper troposphere. Of importance is easterly wind anomaly prevailing within 40°N–40°S in winter, and within subtropical zone in both hemispheres in summer. In particular, East Asian subtropical westerly jet, the most important atmospheric general circulation system in the upper troposphere in the region, weakens obviously from eastern China to the dateline both in winter and summer. Previously, *Haywood et al.* [2000b] briefly mentioned that

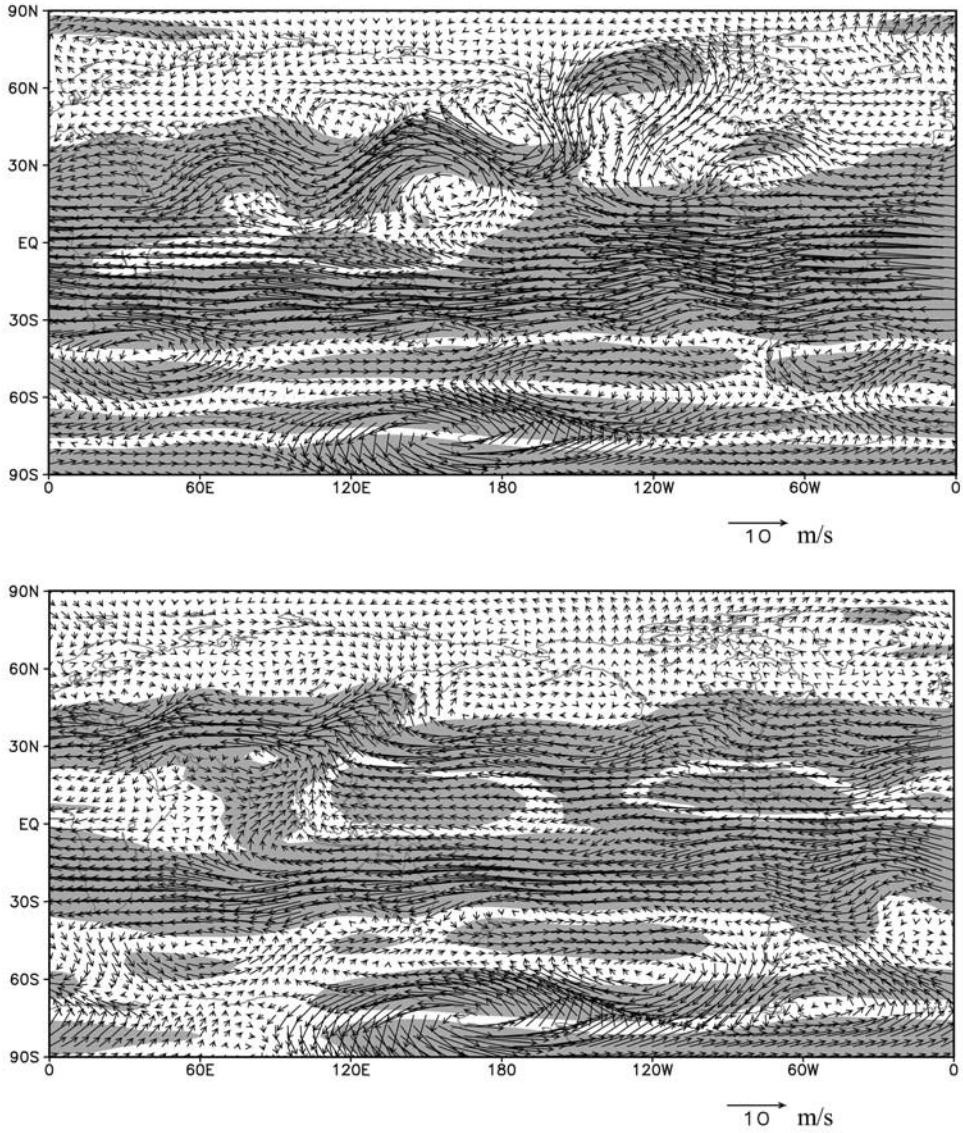

Figure 11. Same as Figure 10, but for 200-hPa wind field. See color version of this figure in the HTML.

the magnitude of the mid-latitude jet stream appears to weaken at the middle Pliocene as reproduced by the UKMO AGCM, although its position does not vary from present day. Thus East Asian jet stream decrease at the interval seems model-independent.

[25] Besides the above horizontal circulation changes, the globally zonally averaged Hadley circulation cell's intensity is reduced at the middle Pliocene, according well with the northern hemispheric case of *Chandler et al.* [1994]. Overall, it is characterized by the weakening rising motion at 5°N–5°S during winter and by both the weakening rising motion in tropics and subsidence over the southern subtropics during summer (not shown). Further investigation shows the East Asian Hadley circulation intensity, averaged within 110–150°E, lessens significantly, especially during winter when the rising and subsidence motion is simultaneously decreased in both hemispheres.

[26] In addition, the integration of Exp3, Exp4, and Exp5 displays the above changes in sea level pressure, wind field at 850-hPa and 200-hPa, and Hadley circulation intensity can be mostly ascribed to the PRISM2 SST and sea ice extent, although the regional influences of reconstructed vegetation and continental ice sheet occur.

4. Comparison Against Model and Data

4.1. Model Comparison

[27] It is of interest to compare the IAP AGCM results with other atmospheric models in order to examine the common and different responses of climate models to the imposed PRISM data sets for the middle Pliocene. First, it should be reminded that only the Northern Hemisphere PRISM (8° × 10°) SST, sea ice extent, and vegetation were used as the GISS AGCM surface conditions [*Chandler et al.*, 1994], whereas the NCAR GENESIS AGCM used the PRISM1 2° × 2° data set to reproduce the middle Pliocene climate [*Sloan et al.*, 1996]. Here, both the boundary conditions and the experimental design in the UKMO

Table 4. Globally Annual Mean Surface Temperature Difference (Unit: °C) and the Precipitation Fraction Value at the Middle Pliocene Relative to the Present in Four Atmospheric Models

	GISS [*Chandler et al.*, 1994]	NCAR GENESIS [*Sloan et al.*, 1996]	UKMO [*Haywood et al.*, 2000b]	IAP (This Study)
Temperature (Northern Hemisphere)	(1.4)	3.6	1.9	2.6 (3.0)
Precipitation (Northern Hemisphere)	(5.1%)	5.0%	6.0%	4.0% (−0.9%)

AGCM study of *Haywood et al.* [2000b] were broadly consistent with that of the IAP AGCM.

[28] The differences of annual mean temperature and precipitation as simulated by the above three atmospheric models and the IAP AGCM are listed in Table 4. It follows that all of the models capture a warmer climate at the middle Pliocene relative to the present. The magnitude of the warming is generally compatible among the models, ranging from 1.4°C to 3.6°C. The geographical distribution of warming is also broadly consistent. All of the above four models reproduce a generally stronger warming at high latitudes, and a relatively weaker warming below 2°C at low latitudes for the NCAR GENESIS AGCM, UKMO AGCM, and IAP AGCM and mostly unchanged at northern low latitudes for the GISS AGCM. In addition, the cooling over most parts of the tropical Pacific, in response to the cold PRISM2 SST, is consistently simulated in the GISS AGCM, NCAR GENESIS AGCM, and IAP AGCM. The vanishing cooling in the UKMO AGCM is most possibly ascribed to the coarse contour interval not displaying anomalies smaller than 0°C. Moreover, the cooling over eastern Africa is consistently reproduced by all of the four atmospheric models. However, intermodel discrepancies are also found. It is particularly noted that warming magnitude is usually smaller at northern high latitudes in the IAP AGCM relative to the NCAR GENESIS AGCM and UKMO AGCM during winter. Additionally, during summer the IAP AGCM simulates a warmer climate in the Northern Hemisphere and a colder climate at 80–90°S compared with the UKMO AGCM.

[29] All of the models reproduce a slightly wetter climate at the middle Pliocene than at present. Annual precipitation enhances on average by 5.1% in the Northern Hemisphere (GISS AGCM), and globally annual precipitation is increased by an average of 6.0% (UKMO AGCM), 5.0% (NCAR GENESIS AGCM), and 4.0% (IAP AGCM) relative to today, respectively. Since the contour interval of precipitation difference is set to 2 mm/day by *Haywood et al.* [2000b], it is difficult to compare precipitation changes between the UKMO and IAP AGCM in detail. However, the UKMO AGCM presents a significantly reduced summer precipitation in East Asia, and an increase over parts of the Qinghai-Tibetan Plateau, which are in good agreement with the changes in the IAP AGCM. Additionally, annual mean precipitation decline in much of East Asia at the middle Pliocene in the NCAR GENESIS AGCM coincides well with the IAP AGCM. It is also noted that East Asian precipitation changes are complex in the GISS AGCM, and no uniform patter is present.

[30] In the presented studies with the above three atmospheric models and the IAP AGCM, the middle Pliocene boundary conditions was adopted directly. Besides the differences of PRISM series data set, the climatological boundary conditions for the control run in these four models differ, complicating the intercomparison of the reproduced middle Pliocene climate. Given the highly nonlinear response of model system to initial atmospheric and boundary conditions, it is hard to uniquely determine the cause-effect relationship in the different simulations. It is therefore recommended that the PRISM group provides uniform boundary conditions for the present climate simulation as this will make future model intercomparison more transparent.

[31] Every model system is characterized by slightly or significantly different dynamical framework, different internal physics processes and parameterizations, different vertical and horizontal resolutions, and so on. Therefore we cannot expect identical results even if climate models are forced by the same internal and external boundary and forcing conditions. However, consistent responses to similar boundary conditions are helpful to assess the reason of past climate changes and consequently to improve our understanding on the present and near future climate changes.

4.2. Model-Data Comparison in East Asia

[32] It should first be mentioned that the RRISM2 data set represents a reconstruction of the ''average'' warmth [*Dowsett et al.*, 1999] within the time period 3.29–2.97 Ma BP according to the geomagnetic polarity timescale of *Berggren et al.* [1995]. Therefore only qualitative model-data comparison is addressed below. Paleoclimatic reconstructions revealed a globally mean warming at the middle Pliocene relative to today, particularly at mid to high northern latitudes, which has been consistently reproduced by the IAP AGCM. Since a global-scale intercomparison of the UKMO AGCM simulation with paleodata [*Haywood et al.*, 2000b] and with the IAP AGCM results (last section) have been addressed, the model-data comparison of the IAP AGCM simulation is limited to East Asia with the reconstructed records not used in creating the PRISM2 boundary conditions.

[33] A pollen study, combined with stable carbon-isotope analysis of organic matter of a fluvio-lacustrine sequence in the Guanzhong basin (109.7°E, 34.4°N) in the central China, indicates that during the period of 3.0–2.7 Ma BP (by polarity timescale of *Berggren et al.* [1995]) persistent steppe vegetation and elephant fossil fauna suggest long-lasting warm and dry climate conditions with little change [*Han et al.*, 1997]. Similarly, a continuously accumulated Yanyu section (109°E, 34°N) of Red Clay and loess-paleosol sequence from the southernmost Chinese Loess Plateau also implied relatively steady warm-dry climate conditions and very likely weak northwesterly winds in winter during 3.0–2.7 Ma BP (by polarity timescale of

Cande and Kent [1995]) [*Han et al.*, 2002]. Furthermore, *Ding et al.* [1998] suggested that the climate during the Pliocene Red Clay formation was continuously warm and humid with relatively small-amplitude oscillations in the Loess Plateau of north-central China.

[34] Weaker-than-today East Asian winter monsoon at the Middle Pliocene is consistently reflected in the Chinese Red Clay and marine sediments. *Ding et al.* [1998] suggested East Asian winter monsoon was generally weak during 5.23–2.58 Ma BP because it is very likely that the aeolian Red Clay was mainly transported by the westerlies, differing significantly from the overlying loess that was transported essentially by the East Asian winter monsoon [*Ding et al.*, 2000]. *An et al.* [2001] reinforced a weak East Asian winter monsoon system during 3.6–2.6 Ma BP and related it to the extent and height of the Himalaya-Tibetan Plateau. Additionally, the marine sediments of ODP site 1143 (9°22′N, 113°17′E) in the West Pacific implied a decreased East Asian winter monsoon system around 3 Ma BP [*Tian et al.*, 2002, 2004, and personal communication, 2005]. Moreover, *Wehausen and Brumsack* [2002], based on the Pliocene sediments from ODP site 1145 (117.5°E, 19°N) in the northern part of the South China Sea, deduced East Asian winter monsoon signal seems to have become slightly weaker ca. 3 Ma BP. Consequently, the middle Pliocene warm-drier climate conditions and decreased East Asian winter monsoon as reproduced by the IAP AGCM (Figures 2, 7, and 10), on the whole, compare favorably to the reconstructed records.

[35] In general, proxies suggested a weak or similar East Asian summer monsoon intensity at the middle Pliocene. Based on the Red Clay and loess-paleosol sequence in Chinese Loess Plateau, *Sun et al.* [1998] and *An et al.* [1999, 2001] deduced an overall weaker-than-today summer monsoon during the whole Pliocene interval. *Ding et al.* [1999] suggested a moderate summer monsoon climate during 3.85–3.15 Ma BP and a generally stronger summer monsoon climate during 3.15 to 2.6 Ma BP (by polarity timescale of *Cande and Kent* [1995], here 3.15 Ma BP is around the middle point of 3.29–2.97 Ma BP). Later, *Ding et al.* [2001] indicated the summer monsoon intensity during 3.4–2.6 Ma BP is comparative to the present. In addition, a weaker-than-today East Asian summer monsoon intensity is presented in the marine sediments from ODP site 1143 [*Tian et al.*, 2002, 2004, and personal communication, 2005]. On the contrary, marine sediments from ODP site 1145 suggested East Asian summer monsoon remained the same or become slightly stronger around 3 Ma BP [*Wehausen and Brumsack*, 2002]. Thus it is difficult to evaluate whether or not data-model is consistent before much more records are reported.

[36] Interestingly, it is recently noted that a study on the sequences of lacustrine sediments indicated a cold-wet episode, with relatively warm-dry and warm-humid intervals, occurred between 3.6 and 2.5 Ma BP in the Yushe and Taigu Basins (around 114°E, 37.5°N), with annual mean temperature being probably 2–6°C lower in the middle to late Pliocene than at present in the middle-eastern Shanxi Plateau of China [*Li et al.*, 2004]. This differs greatly from the interpretation of the above records. The uncertainties in past climatic records just illustrate the need for internally and dynamically consistent paleoclimate modeling of past climate states because numerical model systems can be used as a "laboratory" to address the sensitivity of the climate system to prescribed boundary or forcing conditions and consequently explore the mechanisms responsible for past climate changes.

5. Conclusions

[37] The response of the IAP AGCM to the PRISM2 data set for the middle Pliocene has been investigated. The primary conclusions are as follows:

[38] 1. At the middle Pliocene, globally annual mean surface temperature increased by 2.60°C and terrestrial warming was 1.86°C compared with the present. The warming generally decreased towards low latitudes. In contrast, cooling conditions were registered over parts of the Qinghai-Tibetan Plateau, over most parts of the northern tropical Pacific and the East African rift zone, and at 80–90°S.

[39] 2. The reconstructed SST and sea ice extent are main reason for the middle Pliocene warmth as simulated by the IAP AGCM. The influences due to the PRISM2 reconstructed vegetation and continental ice sheet cannot be neglected in some regions at mid to high latitudes, such as over Greenland, over the Qinghai-Tibetan Plateau, and in the circum-Antarctic, although their individual effects are quite limited on a global scale.

[40] 3. Slightly wetter climate dominated at the middle Pliocene. Globally annual precipitation increased on average by 4.0%, and terrestrial precipitation was 112.5% of the present value. The precipitation enhanced notably at high latitudes, with the augment reaching 33.5% (32.5%) relative to the control run at 60–90°N (60–90°S). On the contrary, drier conditions were registered over most regions between Equator and 30°N. Annual precipitation was significantly reduced in much of East Asia and over the northern tropical Pacific.

[41] 4. At the middle Pliocene, both East Asian summer and winter monsoon systems were significantly decreased relative to the present. *An et al.* [2001], based on the Chinese Red Clay, revealed an overall weaker-than-today East Asian monsoon system during 3.6–2.6 Ma BP and related it to the extent and height of the Himalaya-Tibetan Plateau. However, the IAP AGCM indicates the PRISM2 SST and sea ice extent itself can induce such changes. Therefore particular attention should be paid to oceanic behaviors when exploring the Pliocene climate changes in East Asia.

[42] It is now commonly accepted that there has been a global warming during the 20th century, and that the global emissions of greenhouse gasses will lead to a continued and strengthened warming in the 21st century. Based upon the full range of 35 emission scenarios, a number of climate models have been used to make projections of climate change over the 21st century, and globally averaged surface temperature is projected to increased by 1.4–5.8°C over the period 1990 to 2100 [*Cubasch et al.*, 2001]. However, the spatiotemporal pattern of the warming and the forcing mechanisms responsible for the current and coming warming are highly uncertain. Therefore it is interesting to explore the nature and variability of the middle Pliocene climate because it may be the closest analogy of near future climate during the past 3 Ma.

[43] In general, the middle Pliocene warmth is believed to mainly relate to the increased poleward ocean heat transports [e.g., *Cronin*, 1991; *Rind and Chandler*, 1991; *Crowley*, 1996; *Dowsett et al.*, 1996; *Raymo et al.*, 1996; *Billups et al.*, 1998; *Kim and Crowley*, 2000; *Bennike et al.*, 2002], to slightly increased atmospheric CO_2 concentration [*Crowley*, 1996; *Dowsett et al.*, 1996], to alterations in the cryosphere [*Haywood and Valdes*, 2004], or to combinations thereof. A combination of modeling studies and evidence from the Pliocene fossil flora indicate that the atmospheric CO_2 concentration at 3 Ma BP was not too far from its current level [e.g., *Rind and Chandler*, 1991; *Raymo et al.*, 1996], so it cannot be used to fully account for the middle Pliocene warmth. Therefore the causal factors of the middle Pliocene warming and future climate change are undoubtedly different. However, modeling the middle Pliocene climate is of interest because it can (1) provide insights into the nature of warmer-than-today climate and consequently improve our understanding of processes involved in a warm climate; (2) assess climate model's ability to reproduce a warmer climate; (3) examine the sensitivities of climate models to different forcings and boundary conditions and the associated feedbacks that may be operating in a warm climate regime; and (4) help to interpret the Pliocene geological records.

[44] **Acknowledgments.** The authors would like to sincerely thank Harry J. Dowsett and the PRISM group for kindly providing the latest PRISM2 digital data set. Thanks are due to two anonymous reviewers for the comments which greatly improved the earlier version of manuscript. This study was jointly supported by the Chinese Academy of Sciences under grants KZCX2-SW-133 and KZCX3-SW-221, by the National Natural Science Foundation of China under grant 40405015, and by the Chinese Academy of Sciences' "Hundred Talent" Project (to Yongqi Gao).

References

An, Z. S., et al. (1999), Eolian evidence from the Chinese Loess Plateau: The onset of the late Cenozoic Great Glaciation in the Northern Hemisphere and Qinghai-Xizang Plateau uplift forcing, *Sci. China, Ser. D*, *42*, 258–271.

An, Z. S., J. E. Kutzbach, W. L. Prell, and S. C. Porter (2001), Evolution of Asian monsoons and phased uplift of the Himalaya-Tibetan Plateau since late Miocene time, *Nature*, *411*, 62–66.

Bennike, O., N. Abrahamsen, M. Bak, C. Israelson, P. Konradi, J. Matthiessen, and A. Witkowski (2002), A multi-proxy study of Pliocene sediments from Île de France, north-east Greenland, *Palaeogeogr. Palaeoclimatol. Palaeoecol.*, *186*, 1–23.

Berggren, W. A., D. V. Kent, C. C. Swisher, and M. P. Aubry (1995), A revised Cenozoic geochronology and chronostratigraphy, in *Geochronology, Time Scales and Global Stratigraphic Correlation*, edited by W. A. Berggren et al., *Spec. Publ. SEPM Soc. Sediment. Geol.*, *54*, 129–212.

Bi, X. Q. (1993), IAP 9-level atmospheric general circulation model and climate simulation, Ph.D. thesis, 210 pp., Inst. of Atmos. Phys., Chin. Acad. of Sci., Beijing.

Billups, K., A. C. Ravelo, and J. C. Zachos (1998), Early Pliocene climate: A perspective from the western equatorial Atlantic warm pool, *Paleoceanography*, *13*, 459–470.

Cande, S. C., and D. V. Kent (1995), Revised calibration of the geomagnetic polarity timescale for the Late Cretaceous and Cenozoic, *J. Geophys. Res.*, *100*, 6093–6095.

Chandler, M., D. Rind, and R. Thompson (1994), Joint investigations of the middle Pliocene climate II: GISS GCM Northern Hemisphere results, *Global Planet. Change*, *9*, 197–219.

Clark, P. U., R. B. Alley, and D. Pollard (1999), Northern Hemisphere ice-sheet influences on global climate change, *Science*, *286*, 1104–1111.

Cronin, T. M. (1991), Pliocene shallow water paleoceanography of the North Atlantic Ocean based on marine ostracodes, *Quat. Sci. Rev.*, *10*, 175–188.

Crowley, T. J. (1996), Pliocene climates: The nature of the problem, *Mar. Micropaleontol.*, *27*, 3–12.

Crowley, T. J., and S. K. Baum (1997), Effect of vegetation on an ice-age climate model simulation, *J. Geophys. Res.*, *102*, 16,463–16,480.

Cubasch, U., G. A. Meehl, G. J. Boer, R. J. Stouffer, M. Dix, A. Noda, C. A. Senior, S. Raper, and K. S. Yap (2001), Projections of the future climate change, in *Climate Change 2001: The Scientific Basis, Contribution of Working Group I to the Third Assessment Report of the Intergovernmental Panel on Climate Change*, edited by T. J. Houghton et al., pp. 525–582, Cambridge Univ. Press, New York.

Ding, Z. L., J. M. Sun, T. S. Liu, R. X. Zhou, S. L. Yang, and B. Guo (1998), Wind-blown origin of the Pliocene red clay formation in the central Loess Plateau, China, *Earth Planet. Sci. Lett.*, *161*, 135–143.

Ding, Z. L., S. F. Xiong, J. M. Sun, S. L. Yang, Z. Y. Gu, and T. S. Liu (1999), Pedostratigraphy and paleomagnetism of a ~7.0 Ma eolian loess-red clay sequence at Lingtai, Loess Plateau, north-central China and the implications for paleomonsoon evolution, *Palaeogeogr. Palaeoclimatol. Palaeoecol.*, *152*, 49–66.

Ding, Z. L., N. W. Rutter, J. M. Sun, S. L. Yang, and T. S. Liu (2000), Re-arrangement of atmospheric circulation at about 2.6 Ma over northern China: Evidence from grain size records of loess-palaeosol and red clay sequences, *Quat. Sci. Rev.*, *19*, 547–558.

Ding, Z. L., S. L. Yang, J. M. Sun, and T. S. Liu (2001), Iron geochemistry of loess and red clay deposits in the Chinese Loess Plateau and implications for long-term Asian monsoon evolution in the last 7.0 Ma, *Earth Planet. Sci. Lett.*, *185*, 99–109.

Dowsett, H., R. Thompson, J. Barron, T. Cronin, F. Fleming, S. Ishman, R. Poore, D. Willard, and T. Holtz Jr. (1994), Joint investigations of the middle Pliocene climate I: PRISM paleoenvironmental reconstructions, *Global Planet. Change*, *9*, 169–195.

Dowsett, H., J. Barron, and R. Poore (1996), Middle Pliocene sea surface temperatures: A global reconstruction, *Mar. Micropaleontol.*, *27*, 13–26.

Dowsett, H., J. Barron, R. Poore, R. Thompson, T. Cronin, S. Ishman, and D. Willard (1999), Middle Pliocene paleoenvironmental reconstruction: PRISM2, *U.S. Geol. Surv. Open File Rep., 99-535*. (Available at http://pubs.usgs.gov/openfile/of 99–535)

Felzer, B., T. Webb III, and R. J. Oglesby (1998), The impact of ice sheet, CO_2, and orbital insolation on late Quaternary climates: Sensitivity experiments with a general circulation model, *Quat. Sci. Rev.*, *17*, 507–534.

Fu, C. B., Z. S. An, X. D. Wu, and M. X. Wang (1992), Past climate changes over China (in Chinese), in *Global Change Researches in China*, edited by D. Z. Ye and B. Q. Chen, pp. 3–82, China Earthquake Press, Beijing.

Guo, Q. Y. (1994), Relationship between the variations of East Asian winter monsoon and temperature anomalies in China (in Chinese), *Q. J. Appl. Meteorol.*, *5*, 218–225.

Guo, Z. T., S. Z. Peng, Q. Z. Hao, P. E. Biscaye, Z. S. An, and T. S. Liu (2004), Late Miocene-Pliocene development of Asian aridification as record in the Red-Earth Formation in northern China, *Global Planet. Change*, *41*, 135–145.

Han, J., W. S. Fyfe, F. J. Longstaffe, H. C. Palmer, F. H. Yan, and X. S. Mai (1997), Pliocene-Pleistocene climatic change recorded in fluviolacustrine sediments in central China, *Palaeogeogr. Palaeoclimatol. Palaeoecol.*, *135*, 27–39.

Han, J., W. S. Fyfe, and Z. Gu (2002), Assessment of the palaeoclimate during 3.0–2.6 Ma registered by transition of red clay to loess-paleosol sequence in central north China, *Palaeogeogr. Palaeoclimatol. Palaeoecol.*, *185*, 355–368.

Haywood, A. M., and P. J. Valdes (2004), Modelling Pliocene warmth: Contribution of atmosphere, oceans, and cryosphere, *Earth Planet. Sci. Lett.*, *218*, 363–377.

Haywood, A. M., B. W. Sellwood, and P. J. Valdes (2000a), Regional warming: Pliocene (3 Ma) paleoclimate of Europe and the Mediterranean, *Geology*, *28*, 1063–1066.

Haywood, A. M., P. J. Valdes, and B. W. Sellwood (2000b), Global scale palaeoclimate reconstruction of the middle Pliocene climate using the UKMO GCM: Initial results, *Global Planet. Change*, *25*, 239–256.

Haywood, A. M., P. J. Valdes, and B. W. Sellwood (2002a), Magnitude of climate variability during middle Pliocene warmth: A palaeoclimate modelling study, *Palaeogeogr. Palaeoclimatol. Palaeoecol.*, *188*, 1–24.

Haywood, A. M., P. J. Valdes, B. W. Sellwood, and J. O. Kaplan (2002b), Antarctic climate during the middle Pliocene: Model sensitivity to ice sheet variation, *Palaeogeogr. Palaeoclimatol. Palaeoecol.*, *182*, 93–115.

Jiang, D., H. J. Wang, H. Drange, and X. Lang (2003), Last Glacial Maximum over China: Sensitivities of climate to paleovegetation and Tibetan ice sheet, *J. Geophys. Res.*, *108*(D3), 4102, doi:10.1029/2002JD002167.

Joussaume, S., and K. E. Taylor (1995), Status of the Paleoclimate Modeling Intercomparison Project (PMIP), in *Proceedings of the First International AMIP Scientific Conference*, *Tech. Doc. WMO/TD-732*, edited by W. L. Gates, pp. 425–430, World Meteorol. Organ., Geneva, Switzerland.

Joussaume, S., and K. E. Taylor (2000), The Paleoclimate Modeling Intercomparison Project, in *Proceedings of the Third PMIP Workshop*, *Tech. Doc. WMO/TD-1007*, edited by P. Braconnot, pp. 9–24, World Meteorol. Organ., Geneva, Switzerland.

Kalnay, E., et al. (1996), The NCEP/NCAR reanalysis project, *Bull. Am. Meteorol. Soc.*, *77*, 437–472.

Kim, S. J., and T. J. Crowley (2000), Increased Pliocene North Atlantic Deep Water: Cause or consequence of Pliocene warming?, *Paleoceanography*, *15*, 451–455.

Kohfeld, K. E., and S. P. Harrison (2000), How well can we simulate past climates? Evaluating the models using global palaeoenvironmental datasets, *Quat. Sci. Rev.*, *19*, 321–346.

Li, X. Q., C. S. Li, H. Y. Lu, J. R. Dodson, and Y. F. Wang (2004), Paleovegetation and paleoclimate in middle-late Pliocene, Shanxi, central China, *Palaeogeogr. Palaeoclimatol. Palaeoecol.*, *210*, 57–66.

Liang, X. Z. (1996), Description of a nine-level grid point atmospheric general circulation model, *Adv. Atmos. Sci.*, *13*, 269–298.

Raymo, M. E., B. Grant, M. Horowitz, and G. H. Rau (1996), Mid-Pliocene warmth: Stronger greenhouse and stronger conveyor, *Mar. Micropaleontol.*, *27*, 313–326.

Rind, D., and M. A. Chandler (1991), Increased ocean heat transports and warmer climate, *J. Geophys. Res.*, *96*, 7437–7461.

Sloan, L. C., T. J. Crowley, and D. Pollard (1996), Modeling of middle Pliocene climate with the NCAR GENESIS general circulation model, *Mar. Micropaleontol.*, *27*, 51–61.

Sun, D. H., Z. S. An, J. Shaw, J. Bloemendal, and Y. B. Sun (1998), Magnetostratigraphy and paleoclimatic significance of late Tertiary aeolian sequences in the Chinese Loess Plateau, *Geophys. J. Int.*, *134*, 207–212.

Tao, S. Y., and L. X. Chen (1987), A review of recent research on the east Asian monsoon in China, in *Monsoon Meteorology*, edited by C.-P. Chang and T. N. Krishnamurti, pp. 60–92, Oxford Univ. Press, New York.

Thompson, R. S., and R. F. Fleming (1996), Middle Pliocene vegetation: Reconstructions, paleoclimatic inferences, and boundary conditions for climate modeling, *Mar. Micropaleontol.*, *27*, 27–49.

Tian, J., P. Wang, X. Cheng, and Q. Li (2002), Astronomically tuned Plio-Pleistocene benthic $\delta^{18}O$ record from South China Sea and Atlantic-Pacific comparison, *Earth Planet. Sci. Lett.*, *203*, 1015–1029.

Tian, J., P. Wang, and X. Cheng (2004), Development of the east Asian monsoon and Northern Hemisphere glaciation: Oxygen isotope records from the South China Sea, *Quat. Sci. Rev.*, *23*, 2007–2016.

Toracinta, E. R., R. J. Oglesby, and D. H. Bromwich (2004), Atmospheric response to modified CLIMAP ocean boundary conditions during the Last Glacial Maximum, *J. Clim.*, *17*, 504–522.

Wang, H. J. (1999), Role of vegetation and soil in the Holocene megathermal climate over China, *J. Geophys. Res.*, *104*, 9361–9367.

Wang, H. J. (2002), The mid-Holocene climate simulated by a grid-point AGCM coupled with a biome model, *Adv. Atmos. Sci.*, *19*, 205–218.

Wehausen, R., and H. Brumsack (2002), Astronomical forcing of the east Asian monsoon mirrored by the composition of Pliocene South China Sea sediments, *Earth Planet. Sci. Lett.*, *201*, 621–636.

Wei, J. F., and H. J. Wang (2004), A possible role of solar radiation and ocean in the mid-Holocene east Asian monsoon climate, *Adv. Atmos. Sci.*, *21*, 1–12.

Wyputta, U., and B. J. McAvaney (2001), Influence of vegetation changes during the Last Glacial Maximum using the BMRC atmospheric general circulation model, *Clim. Dyn.*, *17*, 923–932.

Xie, P., and P. A. Arkin (1997), A 17-year monthly analysis based on gauge observations, satellite estimates, and numerical model outputs, *Bull. Am. Meteorol. Soc.*, *78*, 2539–2588.

Zeng, Q. C., C. G. Yuan, X. H. Zhang, X. Z. Liang, and N. Bna (1987), A global grid-point general circulation model, paper presented at WMO/IUGG NWP Symposium, World Meteorol. Soc., Geneva.

Zhang, X. H. (1990), Dynamical framework of IAP nine-level atmospheric general circulation model, *Adv. Atmos. Sci.*, *7*, 66–77.

Zhao, P., X. Zhou, Z. Jian, M. Sparrow, and Y. Han (2004), Modeling the tropical climate and the impact of the western Pacific sea surface temperature at the Last Glacial Maximum, *J. Geophys. Res.*, *109*, D08105, doi:10.1029/2003JD004095.

Z. Ding, Institute of Geology and Geophysics, Chinese Academy of Sciences, Beijing 100029, China.

H. Drange, D. Jiang, X. Lang, and H. Wang, Nansen-Zhu International Research Centre, Institute of Atmospheric Physics, Chinese Academy of Sciences, Beijing 100029, China. (jiangdb@mail.iap.ac.cn)